Eur Biophys J (2009) 38:903–910
DOI 10.1007/s00249-009-0464-7

ORIGINAL PAPER

Intermittent contact mode AFM investigation of native plasma membrane of *Xenopus laevis* oocyte

Francesco Orsini · M. Santacroce · P. Arosio · M. Castagna · C. Lenardi · G. Poletti · F. V. Sacchi

Received: 12 January 2009 / Revised: 12 March 2009 / Accepted: 28 April 2009 / Published online: 21 May 2009

Abstract Intermittent contact mode atomic force microscopy (AFM) was used to visualize the native plasma membrane of *Xenopus laevis* oocytes. Oocyte membranes were purified via ultracentrifugation on a sucrose gradient and adsorbed on mica leaves. AFM topographs and the corresponding phase images allowed for visualization and identification of both oocyte plasma membrane patches and pure lipid bilayer regions with a height of about 5 nm within membrane patches. The quantitative analysis showed a normal distribution for the lateral dimension and height of the protein complexes centered on 16.7 ± 0.2 nm (mean ± SE, $n = 263$) and 5.4 ± 0.1 nm ($n = 262$), respectively. The phase signal, providing material-dependent information, allowed for the recognition of structural features observed in AFM topographs.

Keywords Atomic force microscopy (AFM) · Membrane proteins · Plasma membrane · *Xenopus laevis* oocyte

Introduction

Atomic force microscopy (AFM) is a powerful technique for studying the solid body surface with high spatial resolution. This approach (Binnig et al. 1986) provides measurements of biological samples under physiological-like conditions and has become an important tool for imaging specimens of biological origin, such as individual proteins, nucleic acids, and other biological macromolecules in membranes (Alessandrini and Facci 2005; Muller 2008). Plasma membranes and membrane proteins, whose complex and dynamic organization is largely unknown, are an intriguing research topic. However, it is often found that the structural investigation of eukaryotic membrane proteins by techniques such as X-ray crystallography is hampered by difficulties in protein purification and crystallization. In this framework, AFM offers fruitful and interesting possibilities both at the single protein level and supramolecular complex level (Muller 2008). Intermittent contact mode AFM (Tamayo and Garcia 1996) is an important breakthrough for the application of AFM in biology. In this mode, the dragging forces associated with the lateral movement of the tip during the sample scanning are minimized, thus allowing for the collection of similar repeated images. Moreover, in intermittent contact mode AFM, the phase shift between excitation and response of the cantilever can be used as a material-dependent signal complementary to the topography.

This paper reports an intermittent contact mode AFM investigation of the native plasma membrane of *Xenopus laevis* oocytes. This is a model system in many fields of the life sciences from physiology to biochemistry, embryology, and molecular biology. *X. laevis* oocytes are a well-known, high-efficiency expression system of heterologous membrane proteins, but from the point of view of AFM investigation, their large dimensions (about 1 mm diameter) and the presence of a rich cytoplasmic content (with yolk and granules) represent evident drawbacks in the sample preparation. Here the native plasma membranes of *X. laevis* oocytes were purified by ultracentrifugation on a sucrose gradient and adsorbed on mica leaves

F. Orsini (✉) · M. Santacroce · P. Arosio · M. Castagna · C. Lenardi · G. Poletti · F. V. Sacchi
"Giovanni Esposito" Institute of General Physiology and Biological Chemistry, University of Milan, Via Trentacoste 2, 20134 Milan, Italy
e-mail: francesco.orsini@unimi.it

through a physisorption process. Intermittent contact mode AFM topographs showed both single and double lipid bilayer sheets covered with protein complexes. In addition, the AFM phase signal, simultaneously collected with topography, was helpful in the recognition of structures visualized in the AFM images, allowing for the identification of pure lipid bilayer regions within the membrane patches.

The described approach appears to be applicable for investigating the organization of eukaryotic plasma membrane proteins in a native environment.

Materials and methods

Oocyte preparation

The oocytes were isolated from mature *X. laevis* female frogs and manually defolliculated after treatment with collagenase A (1 mg/mL; Roche, Germany) in the Ca^{++}-free ORII buffer (82.5 mM NaCl, 2 mM KCl, 1 mM $MgCl_2$, and 5 mM Hepes/Tris, pH 7.5) for 30 min at room temperature. Selected V- and VI-stage (Dumont 1972) defolliculated oocytes were maintained at 17°C in Barth's medium [88 mM NaCl, 1 mM KCl, 0.82 mM $MgSO_4$, 0.41 mM $CaCl_2$, 0.33 mM $Ca(NO_3)_2$, and 10 mM Hepes/Tris, pH 7.5] supplemented with 0.005% gentamycin sulfate and 2.5 mM pyruvic acid.

Purification of oocyte plasma membrane by ultracentrifugation

The isolation of the plasma membrane of *X. laevis* oocytes was previously described (Hill et al. 2005). About 300–400 V- and VI-stage defolliculated oocytes were homogenized in oocyte homogenization buffer (OHB) (250 mM sucrose, 5 mM $MgCl_2$, 10 mM Hepes/Tris, pH 7.5; 10 µL per oocyte) by several cycles of pipetting. Homogenates were centrifuged at 500*g* for 7 min at 4°C. Lipids floating on the liquid surface were discarded, and the supernatant was recovered. The pellet was resuspended in the same volume of OHB and rehomogenized as above before centrifugation at 500*g* for 7 min. The supernatant was recovered and combined with the first. A volume of 3 mL of the supernatant was loaded on top of a discontinuous sucrose gradient composed of 50% sucrose in OHB (4 mL) and 20% sucrose in OHB (4 mL) and centrifuged at 30,000*g* for 1 h in a swinging bucket rotor (Beckman). Two major membrane bands were visible, the lower at the interface between 20 and 50% sucrose and the other 1 cm from the top. Each band was then collected, gathered, and diluted threefold in OHB. Total membranes were pelleted at 100,000*g* for 30 min.

Sample preparation for AFM imaging

Membrane sample preparation was described elsewhere (Santacroce et al. 2008). Briefly, purified membranes were carefully washed two times with 1 mL of adsorption buffer (150 mM KCl, 25 mM $MgCl_2$, 10 mM Tris/HCl pH 7.5), resuspended in 1,600 µL of the same buffer and frozen at −80°C until use. Next, 100 µL of resuspended membranes was floated on a freshly cleaved mica leaf. After 90 min of adsorption, the sample was gently rinsed five times with adsorption buffer to remove membranes that had not been adsorbed to the support and finally rinsed twice with deionized water to remove salts. Samples were left to dry in a dust-free environment before measurements.

Atomic force microscopy

Intermittent contact mode AFM measurements were performed using a commercial AFM (Nanoscope Multimode IIId, Veeco) equipped with a 12-µm piezo scanner. Intermittent contact mode AFM operates by scanning a tip, mounted at the end of a vibrating cantilever, across the sample surface so that it is in intermittent contact with the surface; the cantilever amplitude is held constant by altering the vertical position of the scanner. The topography image is then computed from the changes in vertical position. The cantilever vibration also induces phase-signal shifts, which are related to changes in the phase lag of the vibration with respect to the freely vibrating cantilever. These are registered as bright and dark regions as a function of phase; this image mode is referred to as phase imaging. Such images may be controlled to exhibit higher contrast than topography images and can reveal features at the highest resolution. This imaging is not affected by large scan size, and it discloses the fine features of visualized structures, which are sometimes not easily observed in topography images. Phase imaging is recorded simultaneously with topography imaging.

For intermittent contact mode AFM, rectangular silicon probes were used with nominal spring constants around 40 N/m (NT-MDT, Russia) and cantilever lengths of 125 µm. The resonance frequency of the cantilever was about 325 kHz. All imaging was performed in intermittent contact mode using the RMS amplitude of the cantilever as the feedback signal. The RMS free amplitude of the cantilever was on the order of 15 nm and the relative set-point above 95% of the free amplitude. The actual total force applied on the sample during the AFM imaging was approximately 5 nN, as measured by force–distance curve (pull-off step). Images were recorded with a slow scan rate (below 1 Hz) and a resolution of 512 × 512 pixels per image was chosen (i.e., ∽8 min/image).

Image processing and analysis

Original AFM images were flattened by using the Nano-Scope III software (version S.31R1, Veeco) to eliminate background slopes and to correct dispersions of individual scanning lines. Measurements of height and diameter of the protein complexes and membrane lipid bilayers were made using the same software. Diameters were measured at half-height to compensate arbitrarily for tip broadening (Barrera et al. 2008).

Results and discussion

High resolution AFM investigation of membrane proteins needs to be performed on a sample well flattened and firmly adhered to a support. Thus, the success of this approach is strongly related to the development of suitable sample preparation protocols. In the case of *X. laevis* samples, the softness of the oocyte cell prevents its direct visualization by AFM, so the main difficulty concerns the isolation of a clean patch of plasma membrane whose thickness is only about 4 nm (von Heijne and Rees 2008) from this large cell and in the deposition and adhesion of this thin layer onto a flat support. Therefore, sample preparation represented one of the most crucial and challenging points in the AFM study of *X. laevis* oocyte plasma membrane. Recently, this issue has been addressed in some AFM studies reporting different sample preparation protocols to investigate *X. laevis* plasma membranes (Lau et al. 2002; Orsini et al. 2006; Schillers et al. 2000). Here in particular, the native plasma membranes of *X. laevis* oocytes were purified by ultracentrifugation on a sucrose gradient and adsorbed on mica leaves through a physisorption process as detailed in the "Materials and methods".

It worth noting that, although some structural distortions may be induced by air drying, we expect that the arrangement, organization, and dimensions of plasma membrane protein complexes are minimally affected by air exposure as reported elsewhere (Le Grimellec et al. 1995). In addition, previous works have reported that the *X. laevis* oocyte plasma membrane remains undamaged after air exposure (Schillers et al. 2004; Lau et al. 2002).

With these samples, intermittent contact mode AFM investigation allowed us to repeatedly reveal large patches of flattened plasma membrane together with areas without membrane—dark areas in Fig. 1 (I)—that are the mica support. It can be seen that the plasma-membrane patches do not have a uniform organization. Some regions are embedded with protein complexes (II)—the protruding spherical-like structures—whereas others show a very smooth appearance—the bright areas in Fig. 1 (III)—and have been identified as pure lipid bilayers by their height of about

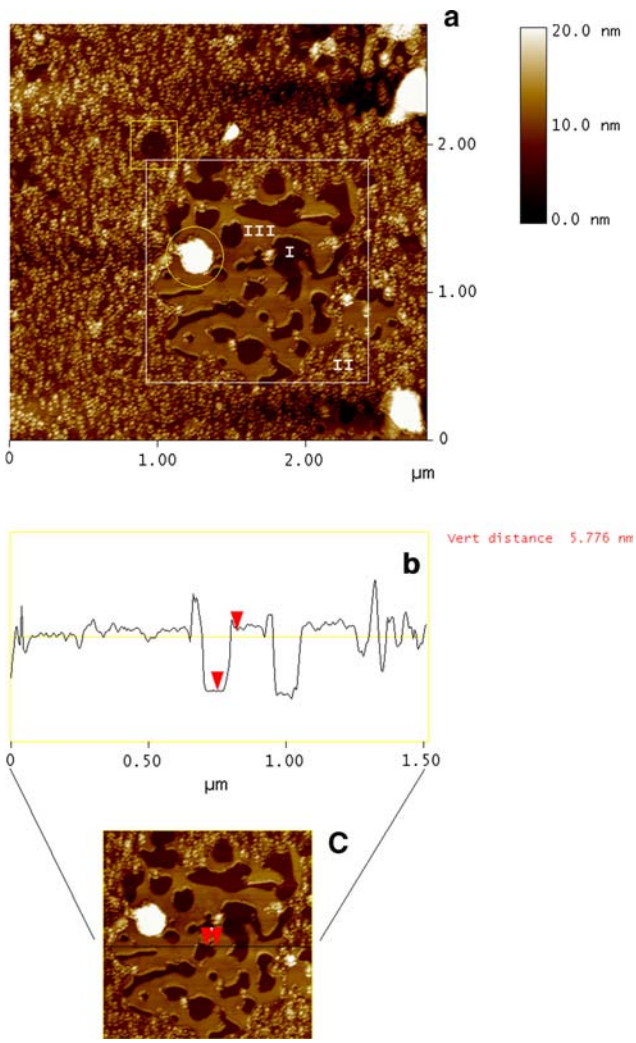

Fig. 1 **a** AFM topography of native plasma membrane of *X. laevis* oocyte adsorbed on a mica support and visualized in air. Three different regions are identified on the sample: mica (darkest areas, *I*), membrane with embedded protein complexes (areas with globular structures, *II*), and pure lipid membrane (brightest and flattened areas, *III*). The *circled area* indicates features higher than 5 nm; the *squared areas* indicate the mica surface. **b** Height profile of the *black line* in **c**. The area in **c** corresponds to the *white box* in **a**. Membrane is present as a single bilayer (height of about 5 nm, see *red arrows*). *Scan area* **a** 2.8 × 2.8 µm^2; Z range (from *darkest* to *lightest*) 20 nm

5 nm. These data are in accordance with previously published data (Schillers et al. 2000) where the lipid bilayer of the *X. laevis* oocyte plasma membrane was measured to be on the order of 5 nm. In the AFM topography image, small areas with relatively high structures, e.g., protein and membrane aggregates and peripheral proteins, are also present.

The edges of membrane patches were used to determine the height of the plasma membrane lipid core and its protruding protein complexes. In particular, the black line drawn in Fig. 1c, corresponding to the profile line reported in Fig. 1b, shows a lipid membrane bilayer with a height of

about 5 nm (see red arrows). Protein complexes protrude from the surface of the lipid bilayer with heights up to 4–6 nm. Proteins appear with different heights and shapes, and some of them are located so close in proximity to each other that they overlap or merge into one structure.

The dimensions of the membrane protein complexes were characterized by analyzing the height profiles of five AFM topographs collected on different samples. The lateral dimension of the complexes showed a normal distribution centered on 16.7 ± 0.2 nm (mean ± SE, $n = 263$), whereas the mean height was 5.4 ± 0.1 nm (mean ± SE, $n = 262$). The distribution of the protein lateral dimension and height values is shown in Fig. 2. The apparent shape of the protein complexes is usually found to be spherical-like, most likely owing to the fact that lateral dimensions of the visualized structures are overestimated as a result of the convolution effect between the structure and the AFM tip (Markiewicz and Goh 1995). The measurements of the protein heights give more reliable values since the vertical resolution of the AFM is better than 0.5 nm and the tip-sample convolution effects are minimized. These results have been compared with the known dimensions of some membrane proteins that show a great variety in shapes and dimensions: some are largely within the membrane lipid bilayer, others have large extracellular regions.

Table 1 reports the heights of some proteins whose structures were recently solved by X-ray crystallography as well as the estimated dimensions of the protein portions protruding from the intracellular or extracellular sides of the membrane hydrophobic core. It is worth noting that these proteins exhibit a height in the range of 5–13 nm and a height for the protruding portion in the range of about 0.5–8 nm (see Table 1). These values are in good agreement with those reported here. The highest values of protein height may be due to the presence of the glycocalyx, a complex structure composed of highly branched sugars that may increase measured heights on the external side of the eukaryotic plasma membrane (Larmer et al. 1997). This is also confirmed by the fact that in Table 1, the eukaryotic organisms have the highest values for extracellular protrusions.

It should be noted that a membrane hydrophobic core thickness of 2.5–3.5 nm can be estimated from Table 1, whereas the smallest value we measured for the lipid bilayer was 5 nm. This last value of course includes the polar heads of phospholipids.

A density of about 350 protein complexes per square micron was calculated. It is interesting to note that a previous contact mode AFM investigation on the same membrane samples, prepared as described here (Santacroce et al. 2008), gave quantitative results comparable with the ones reported above. However, the edges of the visualized structures appear better defined owing to the absence of dragging forces applied to the sample by the AFM tip during the scanning of the sample surface.

Operating in intermittent contact mode, the phase image, obtained by recording the phase shift between excitation and response of the cantilever, can be collected simultaneously to AFM topography. This signal gives material-dependent information complementary to topography to explore various sample properties (e.g., adhesion and viscoelastic properties, capillary forces and wetting) (Stark et al. 2001). Here phase images aided the recognition of structures visualized in the AFM images and were used to identify pure lipid bilayer regions in the oocyte membrane patches.

Figure 3 shows the phase image of *X. laevis* oocyte plasma membrane sheets adsorbed on a mica leaf simultaneously collected with the AFM topography reported in Fig. 1.

Three regions, namely mica (I), oocyte plasma membrane lipid bilayer embedded with proteins (II), and pure lipid

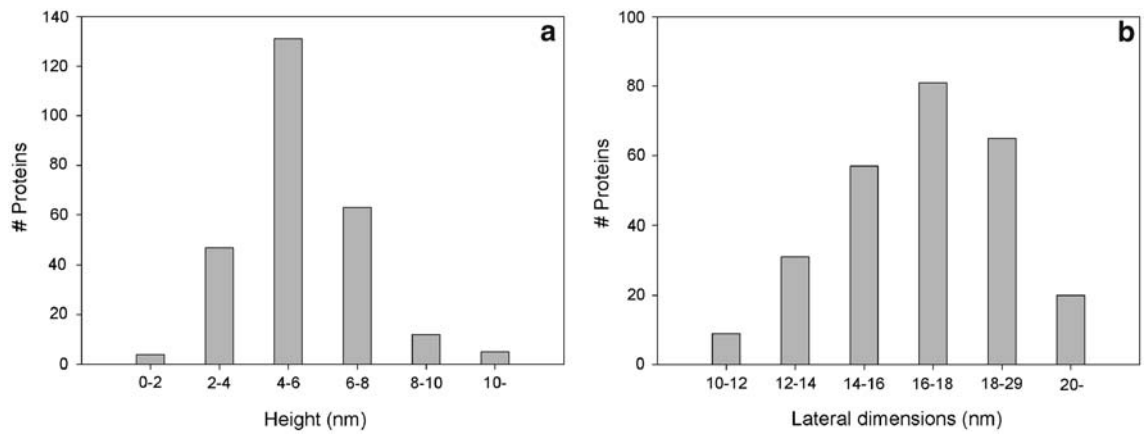

Fig. 2 Histograms of protein **a** height and **b** lateral dimension distribution

Table 1 Height of some membrane proteins whose structure was solved by X-ray crystallography

Reference	PDB ID	Molecule	Source	Height (nm)	Intracellular side (nm)	Extracellular side (nm)
Jasti et al. (2007)	2QTS	Acid-sensing ion channel (ASIC1)	*Gallus gallus*	13[a]	~2[b]	~8[b]
Miyazawa et al. (2003)	1OED	Acetylcholine receptor	*Torpedo marmorata*	~10.5[b]	~0.5[b]	7[a]
Hunte et al. (2005)	1ZCD	Na^+/H^+ antiporter 1 (NhaA)	*Escherichia coli*	5[a]	~0.5[b]	~2[b]
Faham et al. (2008)	3DH4	Na^+/galactose symporter (vSGLT)	*Vibrio parahaemolyticus*	7.5[a]	~1.5[b]	~2.5[b]
Yamashita et al. (2005)	2A65	Na^+/neurotransmitter symporter (LeuTAa)	*Aquifex aeolicus vf5*	7[a]	~1.5[b]	~2[b]
Abramson et al. (2003)	1PV6	Lactose permease (LacY)	*Escherichia coli*	~5.5[b]	~2[b]	~1[b]
Meier et al. (2005)	1YCE	Rotor of F-type Na^+-ATPase	*Ilyobacter tartaricus*	~7[b]	~1.5[b]	~2[b]

The intracellular and extracellular heights of the protein portions protruding from the membrane lipid bilayer were estimated by analyzing the crystal structure drawings when not indicated in the references

[a] Taken from reference

[b] Estimated

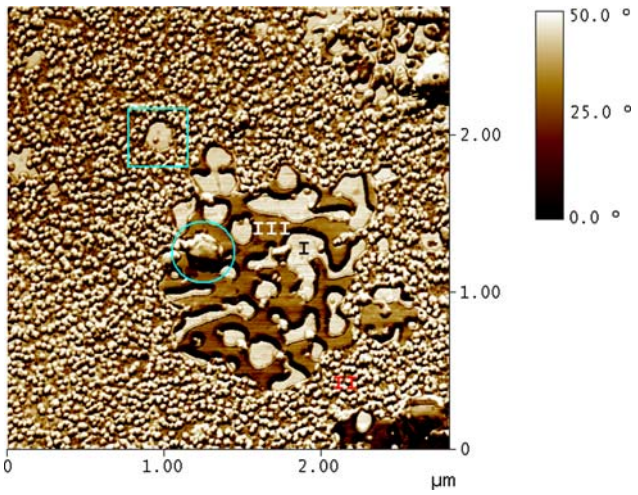

Fig. 3 Phase image of native plasma membrane *of X. laevis* oocyte adsorbed on a mica support and visualized in air. The image was collected simultaneously with the topography reported in Fig. 1. Three different regions are identified on the sample: mica (brightest areas, *I*), membrane with embedded protein complexes (white globular structures, *II*), and pure lipid membrane (darkest and flattened areas, *III*). *Data scale* 50°. *Circled area* indicates lipid membrane multilayer; *squared area* indicates protein complex on mica

membrane bilayer (III), exhibiting a clear contrast are easily identified in Fig. 3. The difference in phase shift between the oocyte membrane lipid bilayer embedded with proteins, the pure lipid area, and mica emphasizes the phase contrast between the materials due to their physical properties.

A shadowing in the scan direction sometimes occurs at positions where large changes are present in the topography, as at step-like features such as the rim of the membrane lipid bilayer and the protein protrusions. At the rising edge, the phase shift is advanced (dark in the image), and at the falling edge it is delayed. It is worth noticing that the interpretation of phase images has to account for influences of the topography, and this is especially important in the case of biological specimens where the surface corrugation is in general the size of the AFM tip. So, in the phase image, the more reliable differences have to be searched for in the smoothest areas where the topography contribution can be considered negligible. In particular, as an example, the phase shifts between mica/pure lipid membrane and mica/membrane lipid bilayer embedded with proteins are given in the line profiles shown in Fig. 4. The phase shift-averaged values for mica/pure lipid membrane and mica/membrane lipid bilayer embedded with proteins are $16.2 \pm 0.5°$ (mean ± SE, $n = 34$) and $3.7 \pm 0.5°$ ($n = 23$), respectively. This difference in phase shift averaged along the scan lines emphasizes the phase contrast between the two different materials.

The phase signal also allows for the recognition of features not easily identifiable in the corresponding AFM topography. In particular, the circled area in the AFM topography reported in Fig. 1 shows a feature with a height much higher than 5 nm. The corresponding phase image identifies, in the same area, the presence of a lipid membrane multilayer (see the color code in the circled area in Fig. 3). In addition, a mica region in the squared area of the AFM topography (see Fig. 1) is shown. The phase signal recognizes a protein complex in the same area (see squared area in Fig. 3).

Using phase images, it was possible to calculate the density of the protein complexes with more accuracy than using topography images. The density value obtained from analyzing phase images was about 10% greater than the one obtained from analyzing topography images. One possible explanation for this discrepancy is that the false-color scale

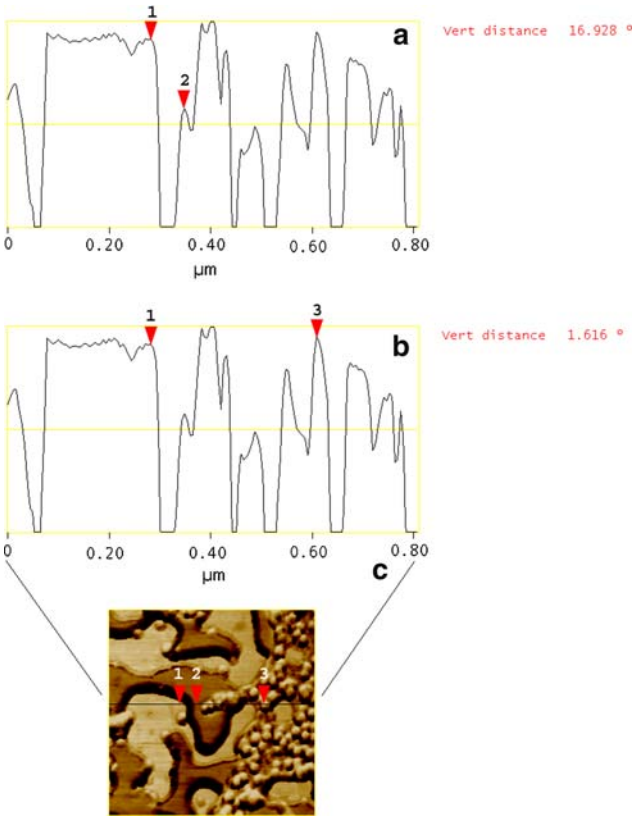

Fig. 4 **a** and **b** Line profiles of the phase image (**c**) of native plasma membrane of *X. laevis* oocyte adsorbed on a mica support. The phase shifts between mica (*1*)/pure lipid membrane (*2*) and mica (*1*)/membrane embedded with proteins (*3*) are shown

of AFM topography images makes some protein complexes less evident with respect to the phase images, whereas protein complexes appear well defined and recognizable.

Since it is not well known how much of the membrane lipid bilayer is occupied by proteins (Engelman 2005), phase signals could help. From this perspective, a viable approach for evaluating the protein coverage would be to discriminate in the phase image a certain range of false-color distribution corresponding to the presence of protein complexes. This implies the selection of appropriate thresholds for defining the lower and the upper limits of the range. This selection is prompted by the presence of a well-defined peak in the histogram representing the false-color distribution. As the number of protruding moieties, correlating with membrane proteins, increases, the better the peak stands out. In the phase image of Fig. 3, we selected different regions of interest showing, at first glance, a homogeneous protein distribution. Thus, by selecting suitable thresholds according to the described criteria, we determined protein coverage to be between 25 and 30% of the oocyte plasma membrane lipid bilayer. It is worth pointing out that this value is related to membrane lipid bilayer regions which are homogeneously populated by proteins. Systematic AFM analysis indicates that all the studied samples also exhibit large areas of pure lipid membrane. Figure 1 is a representative example of typical membrane arrangement. As a consequence of the presence of these regions being depleted in proteins, the mean coverage appears to be lower than the above calculated value.

Finally, a 3D AFM topography image of oocyte plasma membrane collected in a smaller scan area is reported in Fig. 5. The 3D image gives more hints about the three-dimensional spatial structure of the sample. In particular, the higher spatial frequencies, correlating to structural details, are much more evident across the whole vertical range (Raspanti 1999). In addition, 3D rendering can be used to change the viewpoint of the image, providing a better appreciation of the distribution and organization of the protein complexes on the membrane lipid bilayer (see Fig. 5).

AFM is a microscopy technique that allows for the imaging of cellular membranes at molecular spatial resolution and, most importantly to biologists, visualization of biological specimens in buffer solutions and without the need for fixation, staining, or labelling. Moreover, when performed in solution, capillary forces are removed, and thus the AFM tip-sample interactions are reduced, providing softer conditions in which to image the sample. To this end, we performed an investigation of our membrane samples working in a physiological environment. Preliminary data highlighted difficulties relating to the sample preparation, mainly due to both the structural instability of the sample in solution and the sample adhesion to the support. At present, work is in progress to overcome these hindrances by both

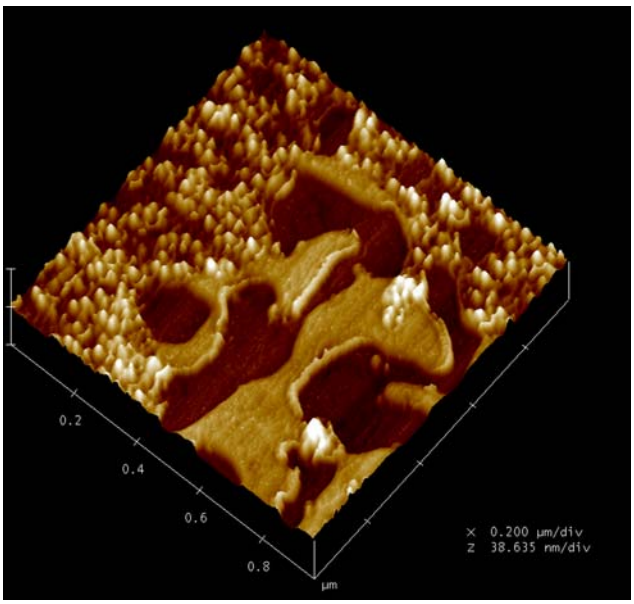

Fig. 5 3D AFM topography of native plasma membrane *of X. laevis* oocyte adsorbed on a mica support. *Scan area* 950 × 950 × 38 nm^3

optimizing some sample preparation parameters, for instance sample adhesion time and membrane concentration, and by using different kinds of support and imaging buffers. Thus far, the most promising results consist of oocyte membrane patches well flattened on a mica support exhibiting a height of about 5 nm and with planar dimensions of approximately a few hundred nanometers—not yet enough to carry out a high resolution AFM investigation (data not shown).

Conclusion

Here we used a sample preparation protocol based on ultracentrifugation on a sucrose gradient for AFM imaging of *X. laevis* oocyte native plasma membranes. Intermittent contact mode AFM and phase signal imaging allowed for the visualization and identification of oocyte membrane lipid bilayers embedded with proteins as well as pure lipid membrane bilayers exhibiting a height of about 5 nm. In particular, by comparing AFM topographs and corresponding phase signals, further details of sample structure have been discussed. The morpho-dimensional characterization of protein complexes visualized on the oocyte native membrane has also been performed, confirming previously published data. For the future, we are aware that only after methodological improvements in sample preparation will it be possible to perform high resolution imaging in a physiological environment with this system. This will also be required for the implementation of more sophisticated investigations with the aim of applying AFM for structural characterization of heterologously expressed membrane proteins and for combining these structural studies with functional studies by means of physiological and biochemical approaches.

Acknowledgments The authors thank Dr. Andrea Cremona for his technical assistance and support given to this work and Dr. Daniel Beck from Warwick University for the revision of the manuscript. This research was funded by grants from the Italian Ministry of Research and University (FIRB programme No. RBNE03B8KK-08) to V.F.S. for the project "Investigation of protein structure and function by AFM and physiological studies."

References

Abramson J, Smirnova I, Kasho V, Verner G, Kaback HR, Iwata S (2003) Structure and mechanism of the lactose permease of *Escherichia coli*. Science 301:610–615. doi:10.1126/science.1088196

Alessandrini A, Facci P (2005) AFM: a versatile tool in biophysics. Meas Sci Technol 16:R65–R92. doi:10.1088/0957-0233/16/6/R01

Barrera NP, Ge H, Henderson RM, Fitzgerald WJ, Edwardson JM (2008) Automated analysis of the architecture of receptors, imaged by atomic force microscopy. Micron 39:101–110. doi:10.1016/j.micron.2006.12.006

Binnig G, Quate CF, Gerber C (1986) Atomic force microscope. Phys Rev Lett 56:930–933. doi:10.1103/PhysRevLett.56.930

Dumont JM (1972) Oogenesis in *X. laevis* (Daudin). Stages of oocytes development in laboratory maintained animals. J Morphol 136:153–180. doi:10.1002/jmor.1051360203

Engelman DM (2005) Membrane are more mosaic than fluid. Nature 438:578–580. doi:10.1038/nature04394

Faham S, Watanabe A, Mercado Besserer G, Cascio D, Specht A, Hirayama BA, Wright EM, Abramson J (2008) The crystal structure of a sodium galactose transporter reveals mechanistic insights into Na^+/sugar symport. Science 321:810–814. doi:10.1126/science.1160406

Hill WG, Southern NM, MacIver B, Potter E, Apodaca G, Smith CP, Zeidel ML (2005) Isolation and characterization of the *Xenopus oocyte* plasma membrane: a new method for studying activity of water and solute transporters. Am J Physiol Renal Physiol 289:F217–F224. doi:10.1152/ajprenal.00022.2005

Hunte C, Screpanti E, Venturi M, Rimon A, Padan A, Michel H (2005) Structure of a Na+/H+ antiporter and insights into mechanism of action and regulation by pH. Nature 435:1197–1202. doi:10.1038/nature03692

Jasti J, Furukawa H, Gonzales EB, Gouaux E (2007) Structure of acid-sensing ion channel 1 at 1.9A° resolution and low pH. Nature 449:316–324. doi:10.1038/nature06163

Larmer J, Schneider SW, Danker T, Schwab A, Oberleithner H (1997) Imaging excised apical plasma membrane patches of MDCK cells in physiological conditions with atomic force microscopy. Pflugers Arch 434:254–260. doi:10.1007/s004240050393

Lau JM, You HX, Yu L (2002) Lattice-like array particles on *Xenopus oocyte* plasma membrane. Scanning 24:224–231

Le Grimellec C, Lesniewska E, Giocondi MC, Cachia C, Schreiber JP, Goudonnet JP (1995) Imaging of the cytoplasmic leafleat of the plasma membrane by atomic force microscopy. Scanning Microsc 9:401–411

Markiewicz P, Goh MC (1995) Simulation of atomic force microscope tip-sample/sample-tip reconstruction. J Vac Sci Technol B 13:1115–1118. doi:10.1116/1.587913

Meier T, Polzer P, Diederichs K, Welte W, Dimroth P (2005) Structure of the rotor ring F-type Na+-ATPase from *Ilyobacter tartaricus*. Science 308:659–662

Miyazawa A, Fujiyoshi Y, Unwin N (2003) Structure and gating mechanism of the acetylcholine receptor pore. Nature 423:949–955. doi:10.1038/nature01748

Muller DJ (2008) AFM: a nanotool in membrane biology. Biochemistry 47:7986–7998. doi:10.1021/bi800753x

Orsini F, Santacroce M, Perego C, Lenardi C, Castagna M, Mari SA, Sacchi VF, Poletti G (2006) Atomic force microscopy characterization of *Xenopus laevis* oocyte plasma membrane. Microsc Res Tech 69:826–834. doi:10.1002/jemt.20353

Raspanti M (1999) Advanced visualization techniques for scanning probe microscopy. Microsc Anal 57:19–21

Santacroce M, Orsini F, Mari SA, Marinone M, Lenardi C, Bettè S, Sacchi VF, Poletti G (2008) Atomic force microscopy imaging of *X. laevis* oocyte plasma membrane purified by ultracentrifugation. Microsc Res Tech 71:397–402. doi:10.1002/jemt.20559

Schillers H, Danker T, Schnittler HJ, Lang F, Oberleithner H (2000) Plasma membrane plasticity of *Xenopus laevis* oocyte imaged with atomic force microscopy. Cell Physiol Biochem 10:99–107. doi:10.1159/000016339

Schillers H, Shahin V, Albermann L, Schafer C, Oberleithner H (2004) Imaging CFTR: a tail to tail dimmer with a central pore. Cell Physiol Biochem 14:1–10. doi:10.1159/000076921

Stark M, Moller C, Muller DJ, Guckenberger R (2001) From images to interactions: high-resolution phase imaging in tapping mode atomic force microscopy. Biophys J 80:3009–3018. doi:10.1016/S0006-3495(01)76266-2

Tamayo J, Garcia R (1996) Deformation, contact time, and phase-contrast in tapping mode scanning force microscopy. Langmuir 12:4430–4435. doi:10.1021/la9601891

von Heijne G, Rees D (2008) Membranes: reading between the lines. Curr Opin Struct Biol 18:403–405. doi:10.1016/j.sbi.2008.06.003

Yamashita A, Singh SK, Kawate T, Jin Y, Gouaux E (2005) Crystal structure of a bacterial homologue of Na^+/Cl^- dependent neurotransmitter transporters. Nature 437:215–223. doi:10.1038/nature03978